

# SURFACE DAMAGE OF ROLLING BEARINGS CAUSED BY DISCRETE CURRENT FLOW

T. ZIKA <sup>1,2</sup>

F. BUSCHBECK <sup>1</sup>

G. PREISINGER <sup>3</sup>

I.C. GEBESHUBER <sup>1,2,4</sup>

M. GRÖSCHL <sup>1</sup>

## 1 INTRODUCTION

### 1.1 Economic background

In recent years, assisted by the promotion of energy-efficiency and alternative energy use, the application of frequency converters to control electric machines (motors and generators) is increasing steadily. Variable speed drive-systems, utilising such control electronics, are capable of saving energy in various applications – especially pumps, fans, electric power engines, lifts ... [1] Furthermore, in the quest for ecological usage of electric energy, wind power is an excellent possibility. Here, due to some beneficial properties, wind power systems using doubly-fed induction generators (DFIGs) are used very commonly [2]. These DFIGs also utilise frequency converters to enable power generation at varying wind speed and, hence, rotor speeds.

### 1.2 Technical background

Despite enabling many energy-efficient driving applications as well as applications for ecological production of electric power, on the far side frequency converters also may provoke reliability problems in the electric machines. The frequency converters usually cause (additional) bearing currents [3] that can harm the bearings of the electric and/or driven machine and, ultimately, may lead to premature failure [4, 5].

In this paper, specially modified bearings are exposed to defined electric stress, similar to what is found in real applications. Only a small number of electric current pulses are applied by discrete electronics during a standardised run on a

---

<sup>1</sup> Institut für Allgemeine Physik, Technische Universität Wien,  
Wiedner Hauptstraße 8-10/E134, 1040 Wien, A; zika@iap.tuwien.ac.at

<sup>2</sup> AC<sup>2</sup>T research GmbH – Österreichisches Kompetenzzentrum für Tribologie,  
Viktor-Kaplan-Str.2, 2700 Wiener Neustadt, A

<sup>3</sup> SKF Österreich AG, Development Cluster Ball Bearings/Technology Development, Seitenstettner Str. 15, 4401 Steyr, A

<sup>4</sup> Institute of Microengineering and Nanoelectronics, Universiti Kebangsaan Malaysia, 43600 UKM, Bangi, Selangor, Malaysia

test rig. The surfaces of the test bearing's rolling elements are then analysed using an atomic force microscope (AFM). Damage to the surface caused by single current pulses is identified for various intensities of current flow. Furthermore, different mechanical operating conditions are compared.

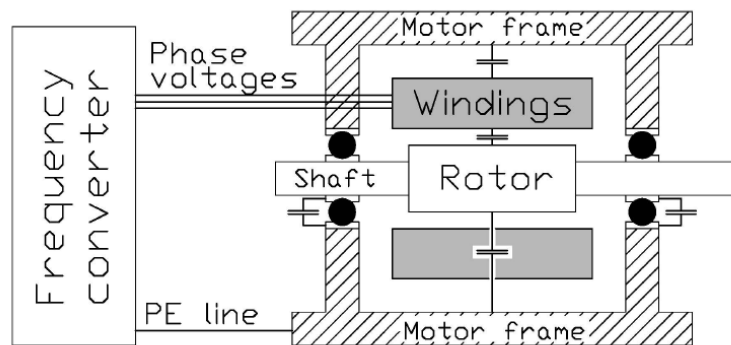


Figure 1: Inherent stray capacitances in a three-phase induction motor driven by a frequency converter.

## 2 TYPES OF BEARING CURRENTS

Apart from classical low-frequency bearing currents, which are known to damage bearings in electric machines for decades [6, 7], electric machines equipped with a frequency converter may suffer from high-frequency currents [8, 9]. These currents are mainly caused by the common mode voltage and the high slew rates of the phase voltage signals delivered by these converters.

The voltage signals delivered to the electric machines are generated by pulse width modulation (PWM) and contain voltage pulses of high slew rates (typically 2-10 kV/ $\mu$ s). This, in combination with inherent parasitic stray capacitances between major elements (e.g. frame to winding ..., see Figure 1) inside the electric machine, causes current flow according to  $I = C \cdot dV/dt$ . Many different current paths are possible inside such a machine. Some of them unfortunately include the bearings, which depending on their actual impedance [10] might eventually get harmed by active current flow. In these modern drive systems the current flow, and hence the deposition of harmful energy, is not continuous anymore, but a discrete process. In worst case it is repeated with every switching operation of the frequency converter.

## 3 EXPERIMENTAL SET-UP

For investigation of the damage done by a single current pulse only, test bearings were exposed to a limited number of current pulses in a test rig. Because of benefits in handling of the tests and of the subsequent analysis thrust ball bearings were used.

The test bearings were modified bearings of SKF type 51305. Instead of nine rolling elements (REs) made of 100Cr6 bearing grade steel only three rolling elements were used: one test rolling element made of electrically conductive bearing grade steel, the two other supporting elements made of insulating silicon nitride as used in hybrid ball bearings (see Figure 2). Subsequently, there was only one distinct current path connecting the two washers of the bearing, namely through the one conductive rolling element. All test bearings were lubricated with the same out-of-the-shelf grease consisting of a mineral base oil and lithium soap thickener. The actual test specimen, which later was analysed, was the one steel rolling element. Therefore, in course of a test series not the whole test bearing was exchanged, but only the steel rolling element was replaced (washers and cage were left unchanged).

### 3.1 Mechanical set-up

The test rig (a sketch of the set-up is depicted in Figure 3), available at SKF Österreich AG and initially designed for testing of standard thrust ball bearings, was modified to enable the application of specific electric regimes to the bearing's washers. The support bearings were hybrid ones; the test rig's shaft (and hence also the shaft washer of the test bearing) was contacted via a rotating mercury contact. A polyamide disk was used to insulate the loaded housing washer against the test rig. The contact to this washer was established by a brass screw going through this insulation layer. Mechanical load was applied using a spring/lever combination and controlled with a load cell.



Figure 2: Test bearing consisting of one steel test RE and two ceramic supporting REs

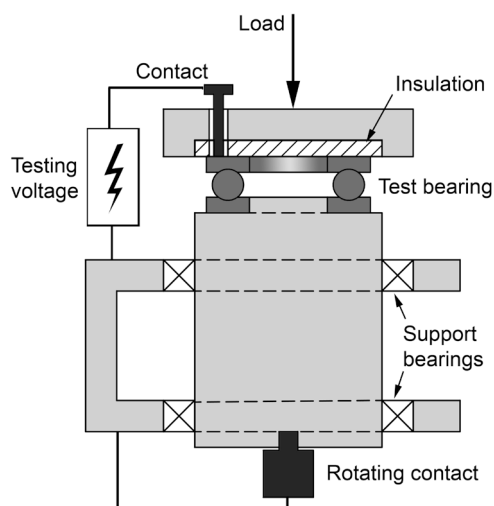


Figure 3: Sketch of the test rig's mechanical set-up

### 3.2 Experimental procedure

A manifold of test runs was carried out with varying rotational speed and electric parameters. The mechanical load, however, and the running times were kept

constant in all those test runs. First of all, a new bearing (more precisely the test bearing equipped with a new rolling element) was mounted onto the shaft. Then it was loaded with an axial force of 400 N. The test bearing (or the new rolling elements) were run-in for 5 minutes without any electric stress being applied. Run-in was followed by application of specific current pulses for 10 minutes. After that, first the current-applying electronics had been disengaged, and then the rotation of the shaft was stopped. The test rig was disassembled until there was free access to the test bearing. Then the housing washer was removed cautiously. The steel rolling element's top position was marked by two scratches. This had been done to later identify a spot on its surface that presumably has been exposed to current flow in the contact zone between rolling element and washer.

### 3.3 Electric regimes

For application of high-frequency pulse currents (HFPCs), specially designed electronics were attached to the bearing. The electronic circuit simulated the current pulses delivered by a frequency converter. The capacitive couplings inside an electric machine were imitated using discrete capacitors. The frequency converter itself was imitated by power transistors applying a square voltage signal to the capacitors, thereby coupling currents to the bearing. Figure 4 shows the principle of this circuit.

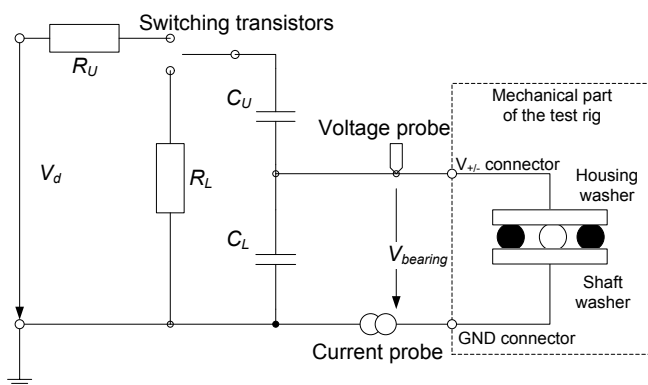


*Figure 4: Operating principle of current-applying electronics*

Like in the real application, the electric energy was applied in a short period of time with comparably long idle periods in between the single pulses. The coupling capacitors ( $C_U$  and  $C_L$ ) are in the order of some nF. The duration of the voltage slope is 100 ns set by the resistors  $R_U$  and  $R_L$ . The pulse repetition frequency in all experiments was rather small compared to modern frequency converters and was in the range of 1-2 kHz.

To vary the intensity of the current pulses, the driving voltage  $V_d$  was set to a specific value between 0 and 30 V. Naturally the voltage applied to the bearing was also affected by this measure. However, it was found to be the better

solution compared to exchanging the coupling capacitors to vary current intensity, because of large tolerances and different frequency behaviour of the different discrete capacitors.

With the terminals of the electronics being short-circuited, variation of the driving voltage results in peak-current values between 0 and approximately 2.5 A (see Figure 5a). In the actual experiment the electric state of the bearing, unsurprisingly, exhibits a great influence on the current passing through (compare Figures 5a and 5b). This is the reason why the applied current pulses cannot be kept uniform. Therefore, in each experiment the current intensities were monitored for a number of events and statistically analysed.

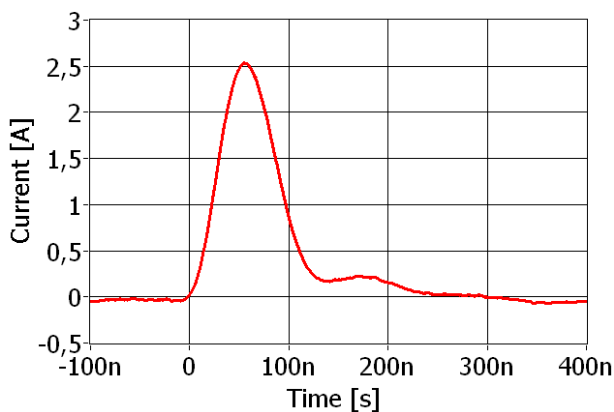


*Figure 5a: Current pulse with short-circuited terminals with  $V_d = 30V$*

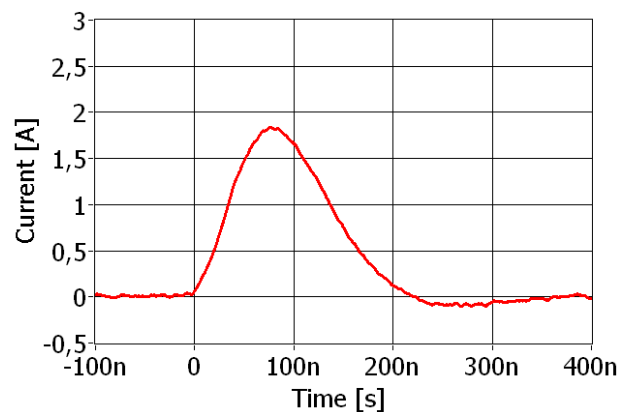


*Figure 5b: Current pulse applied to bearing at 1000 rpm with  $V_d = 30V$*

### 3.4 Analysis of the samples

Analysis of the sample rolling elements was done with an Atomic Force Microscope (AFM). Contact mode was used to record the surface topography and look for damages done by the discrete current pulses applied in the test runs.

Generally, an overview picture of  $80 \times 80 \mu\text{m}^2$  was scanned in the region that had been marked in course of the experimental procedure. One typical feature was then scanned in more detail at  $10 \times 10 \mu\text{m}^2$ .

## 4 RESULTS

Figure 6 shows the topographies of sample rolling elements for 30 V of driving voltage and, as a reference, one without any bearing currents. The current pulses of 500 events were recorded and analysed. This revealed that all three samples were exposed to a peak current of roughly 2.1 A. Average current for the sample with 120 rpm and 60 rpm, respectively, was nearly as high with about 2.0 A. The sample with 1000 rpm showed slightly less average current of 1.9 A.

Still, on its surface only the bearing with 1000 rpm rotational speed (Figure 6a) shows strikingly distinct damage features caused by the electric current passage. The other rolling elements electrically treated at 120 rpm and 60 rpm, respectively (Figure 6b/c), can hardly be distinguished from the sample tested at 60 rpm without any current (Figure 6d).

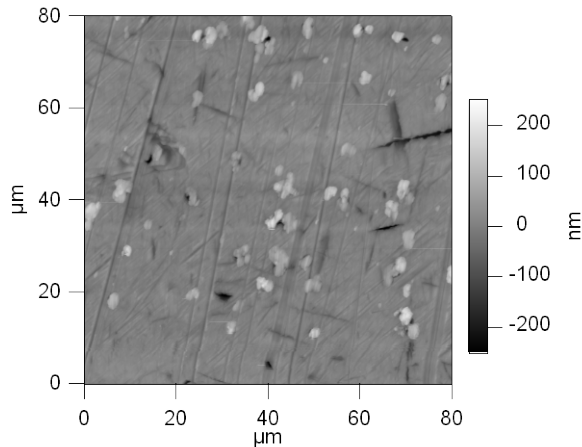


Figure 6a:  $n = 1000 \text{ rpm}$ ;  $V_d = 30 \text{ V}$

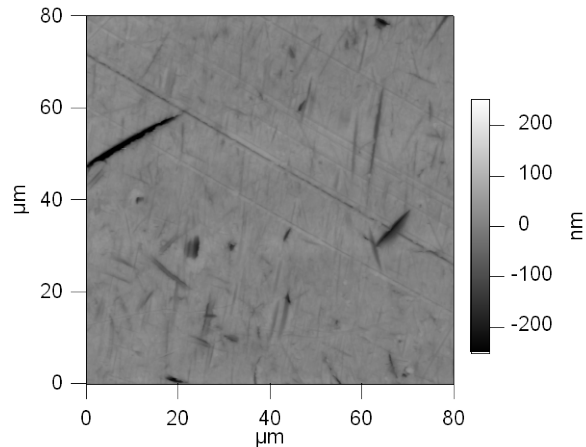


Figure 6b:  $n = 120 \text{ rpm}$ ;  $V_d = 30 \text{ V}$

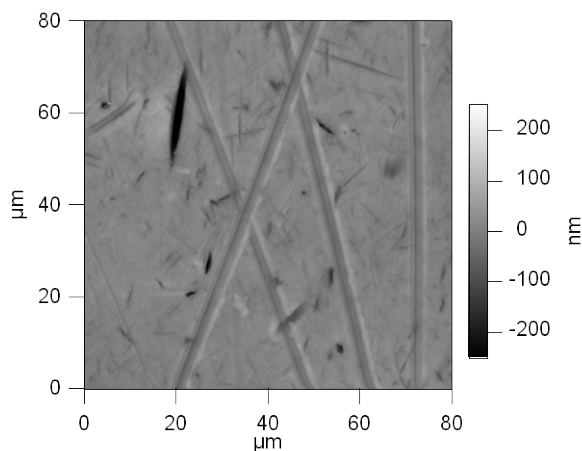


Figure 6c:  $n = 60 \text{ rpm}$ ;  $V_d = 30 \text{ V}$

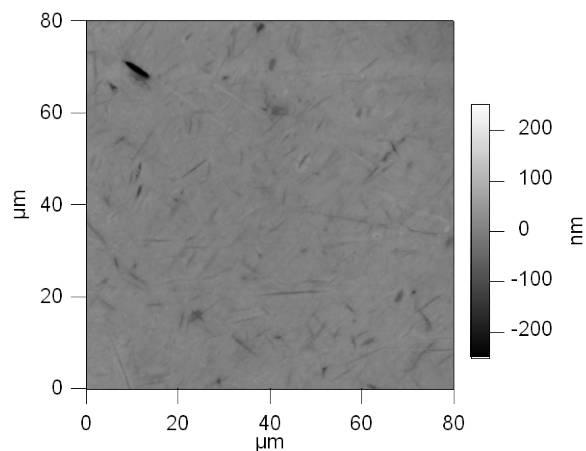


Figure 6d:  $n = 60 \text{ rpm}$ ;  $V_d = 0 \text{ V}$

Figure 6: AFM topography of RE samples created at different rotational speeds

Furthermore samples, all tested using a rotational speed of 1000 rpm, with various electric driving voltages are compared. In Figure 7, single distinct damage features of the surface topography are shown. Generally, the biggest sized features found on the sample surface were chosen for display. These features are more likely created by a current pulse with an intensity similar to the measured maximum current. Based on the topography the extent of the damage is calculated and values for the samples shown in Figure 7 are given in Table 1.

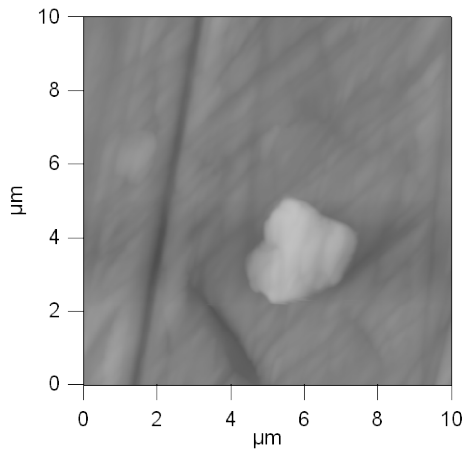
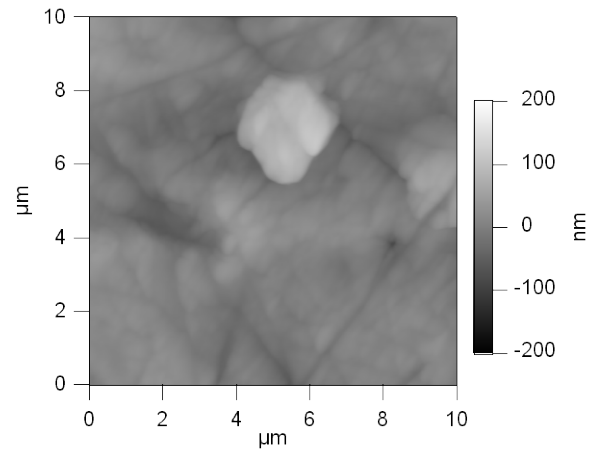
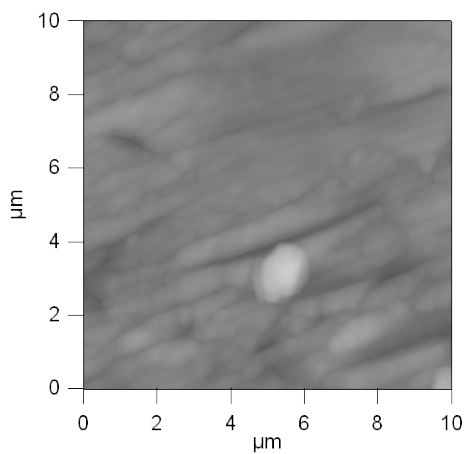
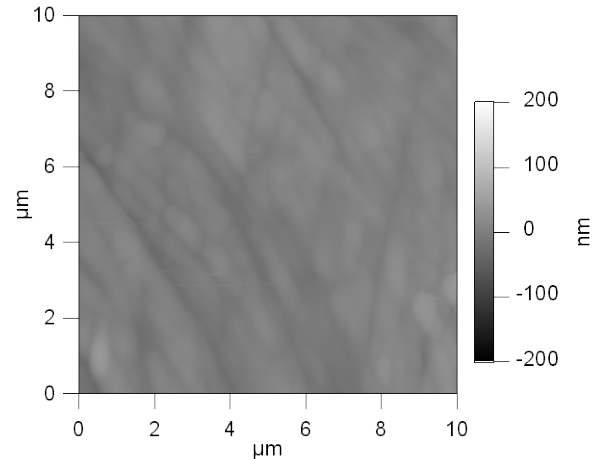

 Figure 7a:  $V_d = 30\text{ V}$ 

 Figure 7b:  $V_d = 20\text{ V}$ 

 Figure 7c:  $V_d = 10\text{ V}$ 

 Figure 7d:  $V_d = 0\text{ V}$ 

Figure 7: AFM topography of RE samples created with different levels of driving voltage and, hence, bearing current intensity. Rotational speed  $n = 1000\text{ rpm}$ .

Sample	Maximum current flow [A]	Approximate diameter [ $\mu\text{m}$ ]	Area [ $\mu\text{m}^2$ ]
$V_d = 30\text{ V}$ (Fig. 7a)	2.17	3.0	5.00
$V_d = 20\text{ V}$ (Fig. 7b)	1.45	3.0	4.92
$V_d = 10\text{ V}$ (Fig. 7c)	0.70	1.6	1.51

Table 1: Measurements of peak current flow and affected area of samples shown in Figure 7

## 5 DISCUSSION

The samples created at 1000, 120 and 60 rpm, respectively, and with a driving voltage of  $V_d = 30V$  (displayed in Figure 6) show that the resulting damage caused by an electric regime clearly differs depending on the bearing's mechanical operating conditions, in this case the rotational speed. Operated at a rotational speed of 1000 rpm (Figure 6a), and therefore in a full-film lubrication regime, the samples show distinct features in their surface topography. This strongly indicates that material has been reworked by the electric current flow. The samples operated at lower rotational speed (120 rpm and 60 rpm) were in a boundary lubrication regime during the test. Here, the AFM topography scan shows no distinguishable features compared to the sample that was operated with no current flow at all. Obviously, the current pulses did not manifest in permanent change of the surface topography, possibly because of better contact (lower resistance compared to the sample run at 1000 rpm) between the washers and the rolling element. Still, damage to the material cannot be fully discarded since other material properties (microstructure, grains, hardness ...) might be affected.

The comparison of samples with different driving voltages and, hence, different current intensities shows the expected trend (Figure 7 and Table 1): the features become bigger in size with increasing current intensity. This is especially valid for the samples with 10 V and 20 V of driving voltage. The difference between the samples with 20 V and 30 V is only marginal. However, it has to be noted that there was no possibility for exact determination of the particular current pulse intensity associated with the displayed craters. So it is not sure that the displayed crater represents one that was created with a current pulse close to the maximum measured value.

## 6 SUMMARY

In practical applications, electric bearing damage is only evaluated after an already huge damage, like micro-cratering (consisting of billions of current pulses) or fluting (a secondary damage) has occurred. This paper for the first time presents the damage done to bearings by single current pulses, similar to those found in modern drive systems comprising frequency converters. It gives a good starting point for further investigation regarding threshold limits and the damaging mechanisms.

## 7 ACKNOWLEDGEMENTS

This work was funded from the Austrian Kplus-Program and has been carried out within the Austrian Center of Competence for Tribology. The authors wish to thank H. Kötttritsch and H. Weninger from SKF Österreich AG, Development Cluster Ball Bearings, for valuable discussions and their support of this work.

## 8 LITERATURE

- [1] de Almeida, A.T., Ferreira, F.J.T.E., and Both, D.: Technical and economical considerations in the application of variable-speed drives with electric motor systems, *IEEE Transactions on Industry Applications*, 41(1), p. 188-199, 2005
- [2] Muller, S., Deicke, M., and DeDoncker, R.W.: Doubly fed induction generator systems for wind turbines, *IEEE Industry Applications Magazine*, 8(3), p. 26-33, 2002
- [3] Hausberg, V. and Seinsch, H.O.: Kapazitive Lagerspannungen und -ströme bei umrichter gespeisten Induktionsmaschinen, *Electrical Engineering*, 82, p. 153-162, 2000
- [4] Mütze, A., Binder, A., Vogel, H., and Hering, J.: Experimental Evaluation of the Endangerment of Ball Bearings due to Inverter-Induced Bearing Currents, *39th IAS Annual Meeting*, 2004
- [5] Zika, T., Gebeshuber, I.C., Buschbeck, F., Preisinger, G., and Gröschl, M.: Surface analysis on rolling bearings after exposure to defined electric stress *Proceedings of the Institution of Mechanical Engineers, Part J: Journal of Engineering Tribology*, 223(5), p. 778-787, 2009
- [6] Andréason, S.: Stromdurchgang durch Wälzlager, *Die Kugellager-Zeitschrift*, 153, p. 6-12, 1967
- [7] Kohaut, A.: Riffelbildung in Wälzlagern infolge elektrischer Korrosion, *Zeitschrift für Angewandte Physik*, 1(5), 1948
- [8] Busse, D., Erdman, J., Kerkman, R.J., Schlegel, D., and Skibinski, G.: Bearing Currents and Their Relationship to PWM Drives, *IEEE Transactions on Power Electronics*, 12(2), 1997
- [9] Chen, S., Lipo, T.A., and Fitzgerald, D.: Source of induction motor bearing currents caused by PWM inverters, *IEEE Transactions on Energy Conversion*, 11(1), p. 25, 1996
- [10] Preisinger, G.: Cause and effect of bearing currents in frequency converter driven electrical motors - investigations of electrical properties of rolling bearings, 2002, TU Wien, Vienna